

Precise Mass Measurement of ^{68}Se , a Waiting-Point Nuclide along the rp Process

J. A. Clark,^{1,2} G. Savard,² K. S. Sharma,¹ J. Vaz,^{1,2} J. C. Wang,^{1,2} Z. Zhou,² A. Heinz,^{2,3} B. Blank,^{2,4} F. Buchinger,⁵ J. E. Crawford,⁵ S. Gulick,⁵ J. K. P. Lee,⁵ A. F. Levand,² D. Seweryniak,² G. D. Sprouse,⁶ and W. Trimble²

¹*Department of Physics and Astronomy, University of Manitoba, Winnipeg, Manitoba R3T 2N2, Canada*

²*Physics Division, Argonne National Laboratory, Argonne, Illinois 60439, USA*

³*Wright Nuclear Structure Laboratory, Yale University, New Haven, Connecticut 06520, USA*

⁴*Centre d'Etudes Nucléaires de Bordeaux-Gradignan, F-33175 Gradignan Cedex, France*

⁵*Department of Physics, McGill University, Montreal, Quebec H3A 2T8, Canada*

⁶*Physics Department, SUNY, Stony Brook University, Stony Brook, New York 11794, USA*

(Received 26 November 2003; published 13 May 2004)

Mass measurements of ^{68}Ge , ^{68}As , and ^{68}Se have been obtained with the Canadian Penning Trap mass spectrometer. The results determine the mass excess of ^{68}Se as $-54\,232(19)$ keV, the first measurement with a precision and reliability sufficient to address the light-curve and energy output of x-ray bursts as well as the abundances of the elements synthesized. Under typical conditions used for modeling x-ray bursts, ^{68}Se is found to cause a significant delay in the rp process nucleosynthesis.

DOI: 10.1103/PhysRevLett.92.192501

PACS numbers: 21.10.Dr, 26.30.+k, 27.50.+e, 98.80.Ft

Consider a binary star system consisting of a red giant and a neutron star. If the neutron star accretes hydrogen and helium from its companion at a rate of $\sim 10^{-9}M_{\odot}\text{yr}^{-1}$, where $M_{\odot} \equiv 1$ solar mass, the gravitational pressure on the material ignites nuclear burning [1], and if the stellar surface becomes sufficiently hot, “break-out” reactions can occur [2]. At this time, the creation of heavier elements is triggered through the rapid fusion of abundantly available protons and nuclides formed from the initial nuclear burning. The resulting energy release is ultimately observed as an x-ray burst [3] which lasts up to 100 s. During this rapid proton-capture process, or rp process [4], the capture rate is favorable compared to the β -decay rate of the nuclides involved, until a nuclide with a small Q value for the proton-capture reaction, Q_p , is reached. Here, an equilibrium between the (p, γ) capture and the competing photodisintegration (γ, p) reactions is established and the rp process stalls until the subsequent β decay of this “waiting-point” nuclide. This equilibrium point depends exponentially on Q_p and therefore the masses of the nuclides involved, most notably ^{64}Ge , ^{68}Se , and ^{72}Kr , are essential to a detailed understanding of the rp process [1,5–8]. For temperatures of 10^9 K which occur in these stellar environments, a mass precision of at least $\text{kT}c^{-2}$ (~ 100 keV c^{-2}) is required. Such a precision is obtained easily with Penning trap mass spectrometers.

As a description of the Canadian Penning Trap (CPT) mass spectrometer has been published previously [9,10], only a brief description of the instrument and details specific to this Letter are presented here. The isotopes ^{68}Ge , ^{68}As , and ^{68}Se were produced in fusion-evaporation reactions between a 220 MeV ^{58}Ni beam [provided by the Argonne Tandem Linear Accelerator System (ATLAS) at the Argonne National Laboratory (ANL)], and carbon targets of 1 mg cm^{-2} (mounted on a rotating target

wheel). The evaporation residues were focused and separated from the primary beam using a combination of a magnetic triplet, a velocity filter, and an Enge split-pole magnetic spectrograph [11]. At the exit of the spectrograph is a gas cell [12], the first element of our gas catcher system, where the ions are thermalized with helium gas. The selected nuclides were accumulated in the gas catcher system and ejected in pulses at a rate of 2 Hz. The ion pulses are then captured in a gas-filled Penning trap ($B \sim 1$ T) and subjected to a mass selective cooling process [13] (resolving power, $\Delta m/m \sim 800$) before being transferred efficiently to a linear RF quadrupole ion trap (RFQ). A fast voltage pulse, applied to one of the beam transport elements, efficiently suppresses isotopes outside a restricted range of masses before being transmitted to the RFQ. The RFQ is used to accumulate several bunches of ions and cool the ions prior to injection into the precision Penning trap for the mass measurement. The total efficiency for the preparation and transport of the ions from the Enge focal plane to the precision Penning trap is typically 2%.

The motion of ions in a Penning trap is described in detail in Ref. [14]. An ion of mass m , subjected only to a homogeneous magnetic field of magnitude B , undergoes cyclotron motion, at a frequency of $\omega_c = qB/m$ where q is the charge of the ion. The ion is confined axially by the addition of an electric field provided by applying an appropriate voltage to the Penning trap electrodes. The resulting electric field in the radial direction, combined with the magnetic field, causes the original cyclotron motion to be split into two eigenfrequencies of radial motion, ω_+ (reduced cyclotron frequency) and ω_- (magnetron frequency), related to ω_c by the following: $\omega_c = \omega_+ + \omega_-$.

The ring electrode of the Penning trap is divided into quadrants to enable the application of azimuthally

oscillating dipole or quadrupole potentials superimposed on the static trapping potential. Ions subjected to a dipole excitation absorb energy resonantly when the driving frequency $\omega_D = \omega_+$ or ω_- . The ω_+ excitation is highly mass selective and is used to remove unwanted isotopes by increasing the radius of the ions' orbit until they are lost from the trap. The ω_- is only weakly dependent on the mass of the ion and is used to establish the initial orbital radius for the desired ions. The influence of a quadrupole excitation is more complicated [15,16] and results in a resonance at ω_c . Since ω_c depends only on the highly stable, homogeneous magnetic field in the Penning trap, precise mass measurements can be obtained by a determination of the cyclotron frequency.

The cyclotron frequency of these ions was determined using the established time-of-flight (TOF) technique [17]. After the excitation frequency has been applied for a prescribed exposure, the ions are ejected from the trap.

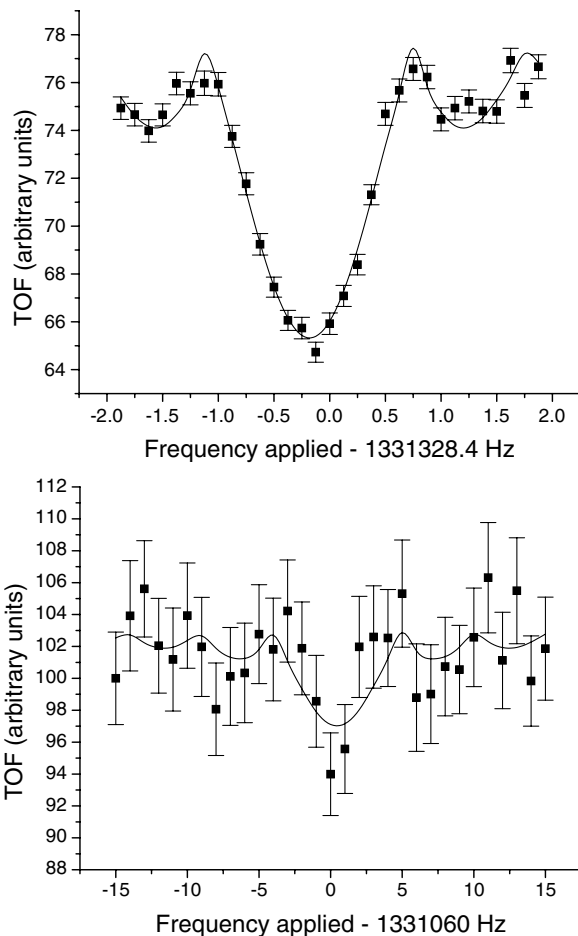


FIG. 1. A TOF spectrum obtained for $^{68}\text{Ge}^+$ (top) and $^{68}\text{Se}^+$ (bottom). A quadrupole excitation of 1000 ms (top) or 200 ms (bottom) in duration was applied after first removing contaminant ions and establishing an orbital radius with a magnetron excitation. The $^{68}\text{Ge}^+$ spectrum has a FWHM of ~ 0.9 Hz (40 keV) and the spectrum shown for $^{68}\text{Se}^+$ has a FWHM of ~ 4.5 Hz (200 keV), consistent with the Fourier limit. The curves shown represent the theoretical line shapes expected.

The radial energy gained from the excitation is then converted into axial energy by their passage through the magnetic field gradient outside the Penning trap. The TOF corresponding to the ions' arrival at a microchannel plate detector is recorded with a multichannel scaler. A TOF spectrum is then generated by plotting the mean TOF of the ions as a function of the driving frequency, where the resonant frequency, ω_c , is obtained by determining the centroid of the spectrum. Calibration spectra are taken periodically, establishing the values of parameters which are used to analyze spectra of low statistics.

Data were obtained from a total of three experimental runs. The first experimental run provided ω_c frequency ratios of $^{68}\text{As}^+$ and $^{68}\text{Ge}^+$ relative to C_5H_8^+ ions (hydrocarbons are produced in the gas catcher system [18]). In the second run, ratios of $^{68}\text{As}^+$ and $^{68}\text{Se}^+$ relative to $^{68}\text{Ge}^+$ were determined. The last run provided ratios of $^{68}\text{As}^+$, $^{68}\text{Ge}^+$, and $^{68}\text{Se}^+$ relative to C_5H_8^+ . Typically, 8 ions per second of $^{68}\text{Ge}^+$, 2.5 ions per second of $^{68}\text{As}^+$, and 0.2 ions per second of $^{68}\text{Se}^+$ were detected at the microchannel plate TOF detector. Shown in Fig. 1 are TOF spectra obtained for $^{68}\text{Ge}^+$ and $^{68}\text{Se}^+$.

The effects of known sources of systematic errors [15] were examined during the course of each measurement. The stability of the magnetic field was checked by periodically measuring ω_c for a reference mass. No shift in magnetic field was detected during a typical three-day experiment within the precision of our measurements. We estimate the effects of such variations as less than 10^{-8} /day. There is a possibility of a small systematic bias, proportional to the difference in mass between the reference mass and the measured species. Since the largest mass difference used in our experiments was only ~ 0.135 u, these effects are negligible since our past measurements [19] indicate that any such effect is less than 10^{-9} /u. Only ion bunches containing few detected ions were used to minimize the effects caused by ion-ion interactions, whether it be interactions between ions of the same nominal mass or of remaining contaminant

TABLE I. Measured values for the cyclotron frequency ratios for each ion measured compared to the indicated calibrant ion. The errors listed are statistical only.

Measured ion	Calibrant	Ratio (R)
^{68}Ge	$^{12}\text{C}_5^1\text{H}_8$	0.998 023 91(12)
^{68}Ge	$^{12}\text{C}_5^1\text{H}_8$	0.998 023 769 4(95)
^{68}Ge	$^{12}\text{C}_5^1\text{H}_8$	0.998 023 811 (16)
^{68}As	^{68}Ge	1.000 128 06(14)
^{68}As	$^{12}\text{C}_5^1\text{H}_8$	0.998 151 12(18)
^{68}As	$^{12}\text{C}_5^1\text{H}_8$	0.998 151 28(14)
^{68}As	$^{12}\text{C}_5^1\text{H}_8$	0.998 151 288 (17)
^{68}As	$^{12}\text{C}_5^1\text{H}_8$	0.998 151 328 (22)
^{68}Se	^{68}Ge	1.000 201 23(40)
^{68}Se	$^{12}\text{C}_5^1\text{H}_8$	0.998 225 14(45)

TABLE II. Constants used in this paper.

Constant used	Value ^a
1 u	931.493 860 MeV c^{-2}
Electron mass	548.580 μu
Mass of $^{12}\text{C}_5^1\text{H}_8$	68 062 600.256 μu

^aObtained or derived from Ref. [20].

ions. Finally, our frequency ratios were taken with roughly the same small number of ions detected for each ion species, with the largest difference being ~ 20 detected ions per ion bunch. This was conservatively estimated to result in a possible systematic error of 40 ppb [19], and is the only systematic error to significantly affect the precision of our results. The final quoted error is a combination of the statistical uncertainty and this systematic error added in quadrature.

Our measured cyclotron frequency ratios from all three runs are given in Table I. For each ratio R , the mass of the neutral isotope, m , is determined using the relationship $m = R(m_c - m_e) + m_e$ where m_e is the mass of the electron and m_c is the mass of the neutral calibrant. In this manner the values in Table I are combined with the auxiliary data in Table II to arrive at the masses shown in Table III. Where more than one value is available for a given mass we have combined them in a weighted average. The values from the 1995 atomic mass evaluation (AME) [20] and the predictions of the finite-range droplet model (FRDM) [21] are also given. Our experimental data show that these nuclei are all more bound (by 539 keV on the average) than predicted by the FRDM, but follow the expected trend based on systematics.

Our value for the mass of ^{68}Se may also be compared with the results of two recent measurements using different techniques [22,23]. Our value agrees with the relatively imprecise value obtained by the SPEG facility [22] [$\Delta M(^{68}\text{Se}) = -53\,620(1000)$ keV]. However, it disagrees significantly with the results obtained from the CSS2 facility [23] [$\Delta M(^{68}\text{Se}) = -52\,347(80)$ keV]. An earlier measurement of the mass excess of ^{68}As [$\Delta M(^{68}\text{As}) = -58\,890(100)$ keV] [24] also agrees with our value. Furthermore, our derived Q_β value for ^{68}Ge [$Q_\beta = -8084.9(41)$ keV] is in excellent agreement with that of Ref. [25] [$Q_\beta = -8100(100)$ keV]. We, therefore, suggest that the result from CSS2 is influenced by previously unconsidered systematic errors.

Our mass determination of ^{68}Se provides a new lower limit for the mass of ^{69}Br . The upper limit of the half-life of this nucleus (24 ns) suggests that it is proton unbound by at least 500 keV [26]. Therefore, the mass excess of ^{69}Br , $\Delta M(^{69}\text{Br}) > \Delta M(^{68}\text{Se}) + \Delta M(p) - Q_p(^{68}\text{Se}) [= -500 \text{ keV}] > -46\,440 \text{ keV}$. The mass excess of ^{69}Br determined from Skyrme Hartree-Fock calculations by Brown *et al.* [$\Delta M(^{69}\text{Br}) = -46\,130(110)$] [7], is in excellent agreement as is the value obtained from the AME [$\Delta M(^{69}\text{Br}) = -46\,410(310)$ keV].

The effective stellar half-life of ^{68}Se , $t_{1/2,\text{eff}}(^{68}\text{Se})$, is a measure of the delay in the rp process at this waiting-point nuclide, with an exponential dependence on $Q_p(^{68}\text{Se})$ as discussed in Ref. [1]. The effect of our mass determination of ^{68}Se on the effective stellar half-life as compared with other groups can be seen clearly in Fig. 2, where typical conditions for x-ray burst models were used (temperature = 1.5 GK, density = 10^6 g cm^{-3} , solar hydrogen abundance, $\langle p\gamma \rangle$ rates taken from Ref. [1]), and the assumption that the photodisintegration of ^{70}Kr is negligible [1]. Under this assumption, the effective half-life of ^{68}Se is determined from its β decay (35.5 s [27]) and the $2p$ -capture rate [see Eq. (44) in Ref. [1]]. The mass measurement of ^{68}Se by CSS2 suggests that the effective stellar half-life of ^{68}Se is less than 1 ms; the relatively imprecise value from SPEG determines the effective stellar half-life to range from less than 1 ms to 34 s. Our precise result, when combined with the mass calculation of ^{69}Br performed by Brown *et al.*, suggests the effective stellar half-life of ^{68}Se is between 29 and 34 s which is consistent with the upper limit of $Q_p(^{68}\text{Se})$ proposed by Pfaff *et al.* [26]. Therefore, the rp process will be slowed down at ^{68}Se , and this has the effect of increasing the abundance of the $A = 68$ elements.

If the photodisintegration of ^{70}Kr is not negligible, then ^{68}Se and ^{70}Kr will establish an equilibrium, and the β -decay rate of ^{70}Kr becomes important in determining the effective stellar half-life of ^{68}Se [1]. The recent ^{70}Kr half-life measurement of 57(21) ms [28] could significantly affect the effective stellar half-life of ^{68}Se if $Q_{2p}(^{68}\text{Se}) = 1.95 \text{ MeV}$ is used as in Ref. [28]. However, the uncertainty in $Q_{2p}(^{68}\text{Se})$ is important since the effective stellar half-life of ^{68}Se is exponentially dependent upon this quantity under the present assumption. Our mass determination of ^{68}Se , when combined with the mass calculation of ^{70}Kr from Brown *et al.* gives $Q_{2p}(^{68}\text{Se}) = 1.33(16) \text{ MeV}$. The effective stellar

TABLE III. Masses of the neutral isotopes with combined statistical and systematic uncertainty, the resulting mass excesses, and comparisons with the AME [20] and FRDM [21].

Nuclide	Mass (μu)		Mass excess (keV)	
	This paper	This paper	AME [20]	FRDM [21]
^{68}Ge	67 928 094.7(29)	-66 979.3(27)	-66 977.0(64)	-66 480
^{68}As	67 936 774.2(33)	-58 894.4(31)	-58 880(100)	-58 460
^{68}Se	67 941 779(20)	-54 232(19)	-54 150(300)	-53 550

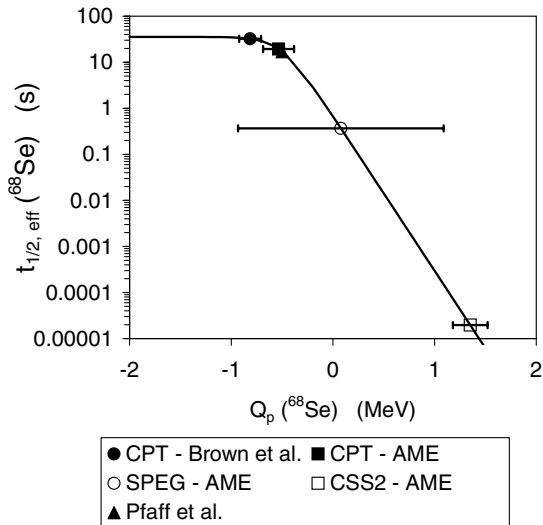


FIG. 2. The effective stellar half-life of ^{68}Se as a function of $Q_p(^{68}\text{Se})$. For the data points with a two-name legend entry, the first name represents the values used for the mass of ^{68}Se , and the second name indicates the value used for the mass of ^{69}Br . Also shown is the upper limit for $Q_p(^{68}\text{Se})$ as determined by Pfaff *et al.* [26]. The curve was calculated under conditions typical for x-ray burst models (temperature of 1.5 GK, density of 10^6 g cm^{-3} , solar hydrogen abundance).

half-life of ^{68}Se is shown in Fig. 3 as a function of the ^{70}Kr half-life for two $Q_{2p}(^{68}\text{Se})$ values, 1.95 MeV as used in Ref. [28], and 1.33 MeV as recommended by us. If our value is used, the effective stellar half-life of ^{68}Se is insensitive to the ^{70}Kr half-life. Furthermore, a $Q_{2p}(^{68}\text{Se})$ of 1.75 MeV would be required to reduce the effective stellar half-life of ^{68}Se by 20%, which is well outside our combined theoretical and experimental uncertainty. We, therefore, believe that the $2p$ -capture rate on ^{68}Se is

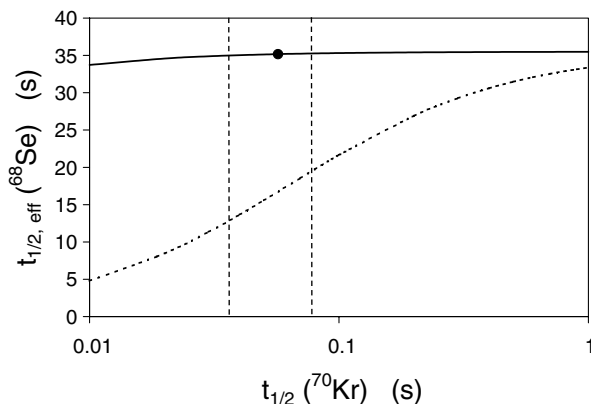


FIG. 3. The effective stellar half-life of ^{68}Se as a function of the half-life of ^{70}Kr for two values of $Q_{2p}(^{68}\text{Se})$: 1.95 MeV (dotted curve) and 1.33 MeV (solid curve). The data point shown indicates the known half-life of ^{70}Kr [28] with its uncertainty represented by the vertical dashed lines.

negligible and that ^{68}Se is truly a waiting-point nuclide and poses a significant delay in the rp process under the assumed conditions.

In summary, x-ray burst models find the mass of ^{68}Se to be an important parameter as they depend exponentially on $Q_p(^{68}\text{Se})$ and $Q_{2p}(^{68}\text{Se})$. We have obtained substantially improved values for the masses of ^{68}Ge , ^{68}As , and ^{68}Se . The masses of ^{69}Br and ^{70}Kr are most reliably obtained by calculations based upon isospin symmetry which inherently cannot provide a mass value of ^{68}Se . Our precise mass measurement of ^{68}Se , in combination with these mass calculations, finds ^{68}Se to be a waiting-point nuclide and presents a considerable delay in the rp process.

This work was supported by the U.S. Department of Energy, Nuclear Physics Division, under Contract No. W-31-109-ENG-38, and by the Natural Sciences and Engineering Research Council of Canada.

- [1] H. Schatz *et al.*, Phys. Rep. **294**, 167 (1998).
- [2] M. Wiescher *et al.*, J. Phys. G **25**, R133 (1999).
- [3] T. Strohmayer and L. Bildsten, in *Compact Stellar X-Ray Sources*, edited by W. H. G. Lewin and M. van der Klis (Cambridge University Press, Cambridge, 2003).
- [4] R. K. Wallace and S. E. Woosley, Astrophys. J. Suppl. Ser. **45**, 389 (1981).
- [5] O. Koike *et al.*, Astron. Astrophys. **342**, 464 (1999).
- [6] H. Schatz *et al.*, Phys. Rev. Lett. **86**, 3471 (2001).
- [7] B. A. Brown *et al.*, Phys. Rev. C **65**, 045802 (2002).
- [8] S. E. Woosley *et al.*, Astrophys. J. (to be published).
- [9] G. Savard *et al.*, Nucl. Phys. **A626**, 353 (1997).
- [10] J. Clark *et al.*, Nucl. Instrum. Methods Phys. Res., Sect. B **204**, 487 (2003).
- [11] J. E. Spencer and H. A. Enge, Nucl. Instrum. Methods **49**, 181 (1967).
- [12] G. Savard *et al.*, Nucl. Instrum. Methods Phys. Res., Sect. B **204**, 582 (2003).
- [13] G. Savard *et al.*, Phys. Lett. A **158**, 247 (1991).
- [14] L. S. Brown and G. Gabrielse, Rev. Mod. Phys. **58**, 233 (1986).
- [15] G. Bollen *et al.*, J. Appl. Phys. **68**, 4355 (1990).
- [16] M. König *et al.*, Int. J. Mass Spectrom. Ion Process. **142**, 95 (1995).
- [17] G. Gräff *et al.*, Z. Phys. A **297**, 35 (1980).
- [18] M. Maier *et al.*, Hyperfine Interact. **132**, 521 (2001).
- [19] J. V. F. Vaz, Ph.D. thesis, University of Manitoba, 2002.
- [20] G. Audi and A. H. Wapstra, Nucl. Phys. **A595**, 409 (1995).
- [21] P. Möller *et al.*, At. Data Nucl. Data Tables **59**, 185 (1995).
- [22] G. F. Lima *et al.*, Phys. Rev. C **65**, 044618 (2002).
- [23] A. S. Lalleman *et al.*, Hyperfine Interact. **132**, 315 (2001).
- [24] M. Hausmann *et al.*, Hyperfine Interact. **132**, 291 (2001).
- [25] R. C. Pardo *et al.*, Phys. Rev. C **15**, 1811 (1977).
- [26] R. Pfaff *et al.*, Phys. Rev. C **53**, 1753 (1996).
- [27] P. Baumann *et al.*, Phys. Rev. C **50**, 1180 (1994).
- [28] M. Oinonen *et al.*, Phys. Rev. C **61**, 035801 (2000).